https://doi.org/10.5194/acp-2021-842
Preprint. Discussion started: 1 November 2021

Atmospheric Chemistry and Physics Discussions

Formation characteristics of aerosol triplet state and coupling effect between the separated components with different polarity

Dongjie Guan[a], Qingcai Chen[a*], Jinwen Li[a], Hao Li[a], Lixin Zhang[a], Yuqin Wang[a], Xiaofei Li[a] and Tian Chang[a]

[a] *School of Environmental Science and Engineering, Shaanxi University of Science and Technology, Xi'an 710021, China*

*Corresponding author:

School of Environmental Science and Engineering, Shaanxi University of Science and Technology, Weiyang District, Xi'an, Shaanxi, 710021, China

*(Q. C.) Phone: (+86) 0029-86132765; e-mail: chenqingcai@sust.edu.cn;

https://doi.org/10.5194/acp-2021-842
Preprint. Discussion started: 1 November 2021

Atmospheric Chemistry and Physics Discussions

Abstract: Atmospheric aerosols contain organic matter that can form triplet state ($^3C^*$) excited by sunlight, which plays a critical role in the aging process of aerosols. In order to understand the triplet state reaction mechanism of complex aerosol components, the formation characteristics of $^3C^*$ in the aerosol components with different polarity, i.e., the highly polar water-soluble matter (HP-WSM), humic-like substances (HULIS) and methanol-soluble matter (MSM) were investigated. The coupling effect of generation of $^3C^*$ and reactive oxygen species (ROS) between different aerosol components was also examined. The results show that the $^3C^*$ generation characteristics is strongly dependent on the polarity of these components. HULIS has the strongest generation ability of $^3C^*$, and the MSM contribute the most to the total generation of $^3C^*$. It is found that the high-energy triplet states ($E_T \geq 250$ kJ mol^{-1}) of HULIS and HP-WSM components account for up to 80%. These $^3C^*$ has an important contribution to the photochemically generation of ROS, and the generated ROS of different components are also different, which is determined by the chromophore composition of complex organic matter. Tyrosine-like chromophore is the main substance leading to the formation of water-soluble $^3C^*$, whilethe highly oxidized HULIS chromophore plays a leading role in the water-insoluble component. This study alos found that there is a coupling effect between HP-WSM and HULIS on $^3C^*$ and ROS generation. The $^3C^*$ generation rate increases by about 40% after mixing, but the generation of $^1O_2$ is severely reduced. Overall, this study provides deep insights into the generation characteristics of the triplet state of atmospheric aerosols.

Key words: atmospheric aerosols; photochemistry; triplet state; reactive oxygen species; coupling effect

TOC:

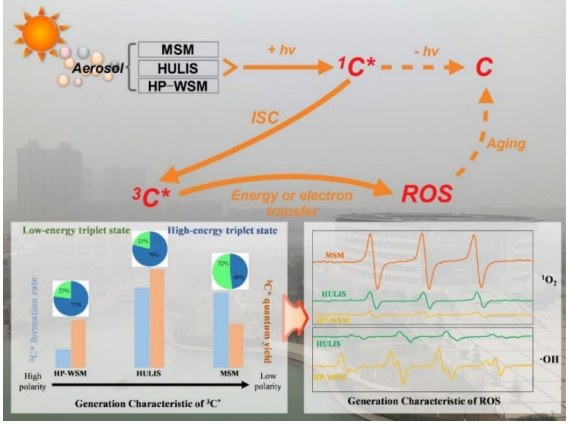

https://doi.org/10.5194/acp-2021-842
Preprint. Discussion started: 1 November 2021

Atmospheric Chemistry and Physics Discussions

1. Introduction

Atmospheric photochemical processes play an important role in the formation and aging of aerosols (Atkinson, 2000; Derwent et al., 1998; Lim et al., 2005; Ervens et al., 2011; Blando and Turpin, 2000). For example, the photo-oxidation process of organic matter and nitrogen oxides affect the cycle of carbon and nitrogen elements (Rollins et al., 2012; Goldstein and Galbally, 2007), and the volatile organic compounds undergo photochemical reactions to generate secondary organic aerosols (SOA) (Griffith et al., 2013; Arce et al., 2008). Part of the photochemical reaction of aerosol is direct photolysis, and in most cases, it is driven by photochemically generated reactive intermediates, including triplet organics ($^3C^*$) and reactive oxygen species (ROS) (Warneck, 1999; Herrmann et al., 2015; Rincon et al., 2009; Lee et al., 2014).

Environmental $^3C^*$ is discovered earlier in natural water, and it has been proven to be an important environmental photochemical reaction intermediate (Vione et al., 2014; Xu et al., 2011). After absorbing solar radiation, this kind of substance will transition from the ground state to the excited singlet state ($^1C^*$), and then rapidly transition to $^3C^*$ through the intersystem. $^3C^*$ directly participates in the degradation of pollutants through the process of energy transfer or electron transfer (Canonica et al., 2006; Parker et al., 2013). It can also indirectly degrade pollutants by generating ROS ($^1O_2$, ·OH, $O_2^{\cdot-}$, $\cdot HO_2$, etc.) (Wenk et al., 2011; Garg et al., 2011; Glover et al., 2013). Because the lifetime of $^1C^*$ is much shorter than that of $^3C^*$, the concentration of $^3C^*$ in the environment is higher than that of $^1C^*$, and the impact of $^3C^*$ on the environment is also greater (McNeill and Canonica, 2016). Compared with the water environment, there are fewer studies on the triplet state in the atmospheric environment. Kaur and Anastasio (2018) used probe technology to conduct photochemical experiments on atmospheric fog droplets and confirmed the existence of $^3C^*$ in the atmospheric environment for the first time. Atmospheric chromophores are organic substances with light-absorbing properties in the atmospheric environment, which are the precursors of $^3C^*$ in aerosols. For example, imidazoles and pyrazines that are widely present in the atmosphere can absorb light radiation to form $^3C^*$ (De-Haan et al., 2010; Hawkins et al., 2018; Laskin et al., 2015). However, because the atmospheric chromophore is not a

https://doi.org/10.5194/acp-2021-842
Preprint. Discussion started: 1 November 2021


Atmospheric Chemistry and Physics Discussions

single substance, but a complex organic mixture, this also increases the difficulty of studying the generation mechanism of $^3C^*$ in actual atmospheric environment.

The environmental organic matter components are composed of complex compounds with different polarities, which are expected to have different optical properties and photochemical reactivity. A study explored the differences in the optical properties of aerosol components with different polarities, and found that substances with lower polarities have a stronger ability to absorb light radiation (Chen et al., 2017). Zhou et al. (2017) separated three organic components of hydrophobic, hydrophilic and transitional hydrophilic (medium hydrophilic) from polluted wastewater, and found a significant difference between $^3C^*$ quantum yield coefficient (f_{TMP}) and singlet oxygen quantum yield (Φ_{1O2}) of each component. $^3C^*$ converts O_2 into $^1O_2$ by means of energy transfer, so this process can be used to determine the energy (E_T) distribution of $^3C^*$, which can be divided into low-energy triplet states (94 kJ mol^{-1} ≤ E_T < 250 kJ mol^{-1}) and high-energy triplet states (E_T ≥ 250 kJ mol^{-1}) (Wilkinson et al., 1993; Kellogg and Simpson, 1965). Zhou et al. (2019) found that high-energy $^3C^*$ accounted for more of the organic matter in water, while soil organic matter had more low-energy $^3C^*$. Although there are some researches on the characteristics of $^3C^*$ formation in water environments, there are very few studies on the characteristics of $^3C^*$ types in the atmospheric environment. Due to the large differences in the sources and chemical processes of organic matter in the atmospheric environment and the water environment, the research conclusions on the $^3C^*$ generation characteristics of water bodies may not be suitable for atmospheric aerosols.

Three-dimensional matrix excitation-emission (EEM) fluorescence spectroscopy technology has been widely used to explore the composition of complex atmospheric chromogenic organic matter (Chow et al., 2004). Chen et al. (2020) used EEM technology to establish the relationship between the atmospheric chromophores and the types and sources of substances, and expanded the application of EEM in the field of atmosphere. The cause of the formation of $^3C^*$ is directly related to the chromophore. Therefore, the EEM method may be conductive to revealing the chemical mechanism of aerosol triplet states. ROS is an important driving factor in the aerosol aging process. Many studies have shown that $^3C^*$ can drive the generation of ROS, and the generation characteristics and mechanisms of ROS by

https://doi.org/10.5194/acp-2021-842
Preprint. Discussion started: 1 November 2021

Atmospheric Chemistry and Physics Discussions

different $^3C^*$ species are not yet known (Vione et al., 2006; Perri et al., 2009;). In summary, in order to explore the formation characteristics and mechanism of triplet in atmospheric aerosols, this study separated complex aerosol components according to polarity, and obtained highly polar water soluble (HP-WSM), humic-like substances (HULIS) and methanol soluble components (MSM, representative of water-insoluble organic matter). Use chemical probe methods (including 2,4,6-trimethylphenol, furfuryl alcohol, and sorbic alcohol) to characterize the generation characteristics of triplet states of different components, including $^3C^*$ generation rate, quantum yield coefficient, and energy distribution (Zhou et al., 2017; Zhou et al., 2019). This study also explored the structure-activity relationship between the type of chromophore and the generation of $^3C^*$, and demonstrated that the generation characteristics and mechanism of ROS depends on the generation of $^3C^*$. Finally, this study confirmed the coupling effect of generation of $^3C^*$ and ROS between different aerosol components (HP-WSM and HULIS).

2. Experimental Section

2.1 Experimental materials

A Mn^{2+} standard in ZnS and Cr^{3+} standard in MgO were purchased from Freiberg Instruments Inc., Delfter, Germany. Glucose (≥99.5%), 4-Hydroxy-2,2,6,6-tetramethylpiperidine (TEMP, ≥98%), L-Histidine (≥99%), Phenol (≥99.5%), 2,4,6-Trimethylphenol (TMP, ≥98%), Furfuryl alcohol (FFA, 98%) and 5,5-Dimethyl-1-pyrroline-N-oxide (DMPO, 97%) were purchased from Aladdin Reagent Company (Shanghai, China). Trans, trans-2,4-hexadien-1-ol (Sorbic alcohol, 97%) was purchased from Sigma-Aldrich. 4-Nitroanisole (PNA, ≥99%) was purchased from Thermo-Fisher. Pyridine (pyr, ≥99%) was purchased from Alfa-Aesar. C18 cartridge (500 mg/6 mL) was obtained from Agela Technologies. All chemicals were used as received.

2.2 Sample collection and preparation

Atmospheric $PM_{2.5}$ samples were collected in Xi'an city, China during the winter from 2019.12.21 to 2020.2.1 (Sample list is shown in **Table** S1). The sample collection point was located on the top of Shaanxi University of Science and Technology, about 40 m above the ground. A large flow sampler (XT-1025, Shanghai Xintuo, China) was used to collect

https://doi.org/10.5194/acp-2021-842
Preprint. Discussion started: 1 November 2021


Atmospheric Chemistry and Physics Discussions

atmospheric particulate samples for 23.5 hours. The samples were collected on a 20×25 cm quartz membrane pre-fired in a muffle furnace (2500 QAT-UP, Pallflex Products Co., US), then the collected sample film is stored at -20 ℃ until use. The simulated combustion PM samples include wheat straw, rice straw, poplar wood, bituminous coal, and lignitous coal. The combustion samples were prepared through a self-built combustion-gas-gathering device. The final particles were collected on a 47 mm diameter quartz membrane and stored at -20 ℃ (**Text S1** for specific sample collection process and sample information).

The samples were continuously extracted with water and methanol ultrasonically for 20 minutes, and then filtered with a 0.45 μm PTFE filter to obtain the water-soluble extract (WSM) and methanol extract (MSM), respectively. Note that the MSM here does not actually contain water-soluble substances, thus it represents water-insoluble organic matter. Then, according to the previous method,the solid-phase extraction technology was used extract HP-WSM and HULIS from WSM (Lin et al., 2012; Chen et al., 2016), as shown in **Text** S1 (the separation process) and **Table** S3 (sample component information). The final concentration of all solution samples after dilution or concentration is controlled to 20 mg-C L^{-1}, and stored at 4 ℃ for later use.

2.3 Organic carbon (OC)/elemental carbon (EC) analysis

Both original sample films and the prepared sample solution were used for the analysis of organic carbon (OC)/elemental carbon (EC), and an OC/EC analyzer (Model 4, Sunset, America) with IMPROVE_A temperature protocol was employed for quantitative analysis. The original sample was directly measured with a 6 mm diameter filter membrane, and the sample solution was subjected to OC/EC analysis by loading 100 μL of the solution onto the 17 mm diameter membrane, and then drying the solvent with nitrogen blowing. The background filter sample was also processed and analyzed with the same procedure, and the background signal interference was subtracted from the final result.

2.4 Spectroscopic characterization

The sample's absorption spectrum and fluorescence spectrum were obtained at the same time in the "fluorescence + absorbance" mode by an Aqualog EEM analyzer (Horiba Scientific, USA). In order to reduce the influence of internal filtration effect on EEM measurement, the solution sample used for optical analysis was diluted before analysis. The

https://doi.org/10.5194/acp-2021-842
Preprint. Discussion started: 1 November 2021


Atmospheric Chemistry and Physics Discussions

concentration of the solution during analysis is shown in **Table** S4. The instrument analysis parameters are set as follows: excitation wavelength of 200-600 nm, emission wavelength of 250-800 nm, scanning interval of 2 nm and exposure time of 1 s. The background sample was also analyzed in the same way and subtracted from the actual sample spectrum. A total of 80 sample EEM spectra were analyzed through the PARAFAC model to identify the chromophore types. According to the change trend of the minimum residual error of the 2-7 component PARAFAC model (**Fig.**S10) and the interpretability of the chromophores to the actual meaning, finally 4 component model was used (**Fig.**S11).

2.5 Photochemical experiments

The sunlight is simulated by a 300 W xenon light source (PLS-SXE 300, Perfectlight, China) and equipped with a VISREF filter. By combining a cold water circulation machine and a magnetic stirrer, the experiment temperature is kept at about 25 °C. The sample solution (120 μL) added with the chemical probe is placed in a special quartz reaction dish (diameter 12 mm, thickness 2 mm) for light reaction, setting a series of light time and taking samples at specific time intervals to perform HPLC analysis (**Text** S2 for lighting equipment and specific steps). A blank control was performed during the experiment, and 3 parallel experiments were set up in each group.

2.6 ^{3}OM and $^1O_2$ measurements and calculation of quantum yields*

In order to determine the production of ^{3}C* and $^1O_2$, TMP (20 μM) and FFA (20 μM) were used as capture agents for ^{3}C* and $^1O_2$, respectively (Halladja et al., 2007; Dalrymple et al., 2010). The two capture agent solutions have almost no loss under the direct irradiation of the light source (**Fig.**S7). The probe concentration was analyzed by a high performance liquid chromatography (LC-100, WuFeng, Shanghai) equipped with a C-18 column (4.6×250 mm, 5 μm, Xuanmei). The acetonitrile (ACN) and ultrapure water were used as the mobile phase, and the flow rate is 1 mL min^{-1}. The detection condition of TMP is mobile phase ACN/Water = 50/50, and the detection wavelength is 210 nm; while for FFA, the related terms are 30/70 and 219 nm, respectively.

The sorbic alcohol (1 mM) is used as a high-energy quencher to quench high-energy ^{3}C* (Zhou et al., 2017a), and combine the Φ_{1O2} to quantify the energy distribution of different ^{3}C*. The reaction consumption rate of TMP (k_{TMP}) and the calculated quantum

https://doi.org/10.5194/acp-2021-842
Preprint. Discussion started: 1 November 2021

Atmospheric Chemistry and Physics Discussions

yield coefficient (f_{TMP}) of the triplet state are used to reflect the $^3C^*$ generation rate and ability. According to previous articles, the Φ_{1O2} and f_{TMP} are calculated as follows (Dalrymple et al., 2010; Bodhipaksha et al., 2015; Mostafa and Rosario-Ortiz, 2013).

$$\phi_{^1O_2} = \frac{R_{^1O_2}}{R_a} \quad (1)$$

$$f_{TMP} = \frac{k_{TMP}}{R_a} \quad (2)$$

$$R_a = \sum_\lambda \frac{I_\lambda(1-10^{-la_\lambda})}{l} \quad (3)$$

$$R_{^1O_2} = \frac{k_{FFA} \times k_d}{k'_{FFA}} \quad (4)$$

$R_{^1O_2}$ is the rate of generation of singlet oxygen (M s^{-1}); R_a is the light absorption rate (einsteins cm^{-3} s^{-1}); k_{TMP} and k_{FFA} are the pseudo-first order reaction rate constant consumed by TMP and FFA (s^{-1}); I_λ is the photon flux at λ wavelength (Einsteins cm^{-2} s^{-1} nm^{-1}), as shown in S3 for specific calculation; a_λ represents the unit absorbance of the solution at the wavelength of λ (cm^{-1}); l is the thickness of the solution (0.1 cm); k'_{FFA} is the rate constant of $^1O_2$ and FFA reaction (1.2×10^8 M^{-1} s^{-1}); k_d is the rate constant of water quenching $^1O_2$ (2.4×10^5 s^{-1}). The wavelength range of light radiation for calculation in this study is from 320 nm to 600 nm.

2.7 Reactive oxygen detection ($^1O_2$, ·OH)

In order to explore the characteristics and mechanism of ROS generated by $^3C^*$, the combination of free radical capture technology and electron paramagnetic resonance spectrometer (EPR, MS5000, Freiberg) was used to detect two ROS including $^1O_2$ and ·OH. The concentration of the experimental sample solution is controlled to 100 mg-C/L, using TEMP as $^1O_2$ capture agent, DMPO as a capture agent for ·OH. The concentration of the capture agent after mixing is 10 mM. When capturing $^1O_2$, the illumination time is 60 min, and when capturing ·OH, the illumination time is 10 min. At the same time, the 0 point of illumination is set upand the non-illumination control group is carried out. In this study, Sorbic alcohol and histidine (both 50 mM after mixing) were used as quenchers of $^3C^*$ and $^1O_2$, respectively, to explore the generation mechanism of $^1O_2$ and ·OH.

https://doi.org/10.5194/acp-2021-842
Preprint. Discussion started: 1 November 2021


Atmospheric Chemistry and Physics Discussions

The EPR detection parameters for the $^1O_2$ and ·OH are the same: magnetic field strength, 330-342 mT; detection time, 180 s; modulation amplitude, 0.2 mT; number of detections, 1; and microwave intensity, 8.0 mW.

3. Results and Discussion

3.1 Carbon composition of different polar aerosols

Organic carbon is the main precursor for the formation of triplet states in aerosols, and the composition of organic carbon is different between components of different polarities. The results of carbon analysis are shown in **Fig.**1. The OC values of environmental $PM_{2.5}$ samples in winter is in the range of (19.51-44.97) μg-C/m^3, of which the WSOC component accounts for about half of the OC, mainly the HP-WSOC component (25%-37%). The average concentration of HULIS-C in this study is (3.39±1.38) μg·C/m^3, and the concentration is between clean areas and areas severely affected by biomass burning (Nguyen et al., 2014; Wang et al., 2017). Affected by source and environmental conditions, the composition and concentration of HULIS vary greatly, generally accounting for 8-74% of WSOC (Feczko et al., 2007). In this study, HULIS accounts for 26% of WSOC, which is at a moderate level. The water-insoluble organic matter MSOC accounts for about 20% of the OC of the $PM_{2.5}$ sample. This result indicates that there is a considerable part of the water-insoluble organic carbon in the particulate sample. It is worth noting that the content of water-insoluble organic carbon may be higher, considering that 34% of the organic carbon has not been extracted (**Fig.**1 b1).

The MSOC in the primary combustion sample is generally higher than that in the actual PM sample. In the biomass sample, 35%-64% of the components in OC are MSOC, while the HP-WSOC and HULIS in OC are basically the same at 19%-22%. There are very few water-soluble components in coal combustion samples. Nearly 90% of OC components are MSOC. MSOC should be macromolecular organics, especially tar-like substances formed during coal combustion. Whether it is coal combustion or biomass combustion, the content of coking organic carbon in thermo-optical analysis is significantly higher than that of actual atmospheric samples (**Fig.**S11).

https://doi.org/10.5194/acp-2021-842
Preprint. Discussion started: 1 November 2021

Atmospheric Chemistry and Physics Discussions

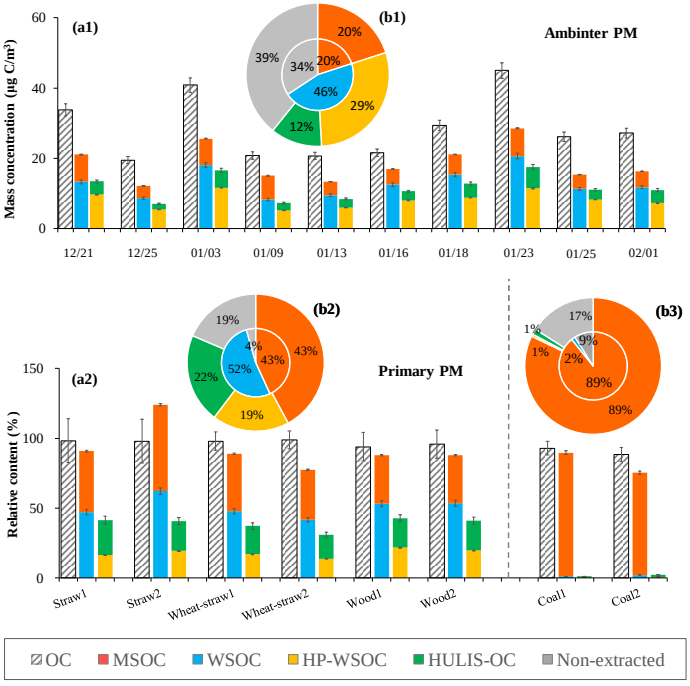

Fig.1 The content of organic carbon in different polar components of atmospheric aerosol. (a1) and (a2) represent the organic carbon content in actual atmospheric aerosol samples and primary combustion source samples, respectively; (b1), (b2) and (b3) represent the average relative content of organic carbon of different polarity groups in actual atmospheric aerosols, biomass combustion aerosols, and coal combustion aerosol samples, respectively. The error bars represent the relative standard deviations obtained for a set of three parallel samples.

3.2 Triplet generation ability of aerosols with different polarities

The characteristics of triplet generation of components with different polar in aerosol are different. The pseudo-first order reaction kinetic rate constant k_{TMP} of the triplet state and TMP is usually used to characterize the rate of formation of $^3C^*$, and the triplet quantum yield coefficient (f_{TMP}) reflects the ability of the triplet state to be generated (Ervens et al., 2011; Zhou et L., 2017b). **Fig.**2(A)(B) shows the average attenuation curve and average k_{TMP} value of the reaction of different components with TMP under illumination conditions. The k_{TMP} of each sample is shown in **Table** S5, and the average TMP attenuation fitting curve is shown in **Fig.**S16. The results show that the aerosol components with different polarities exhibit different generation rates of $^3C^*$. The k_{TMP} of the components with different polar in the actual PM sample is between 0.004-0.017 min^{-1}, and the k_{TMP} of the HP-WSM component is the lowest. In the biomass combustion samples, all polar components did not

https://doi.org/10.5194/acp-2021-842
Preprint. Discussion started: 1 November 2021

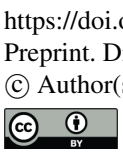

Atmospheric Chemistry and Physics Discussions

significantly consume TMP; although HP-WSM in coal samples did not consume TMP, HULIS and MSM components were consumed significantly, with an average k_{TMP} value of 0.054 min^{-1}. **Table** 1 lists the f_{TMP} values of the components with different polar of each sample. The f_{TMP} value of the HULIS component of the atmospheric PM sample is between (35-180) M^{-1}, which is higher than the HP-WSM component (5-90) M^{-1} and MSM component (14-70) M^{-1}, indicating that the HULIS has the strongest ability to generate triplet states.

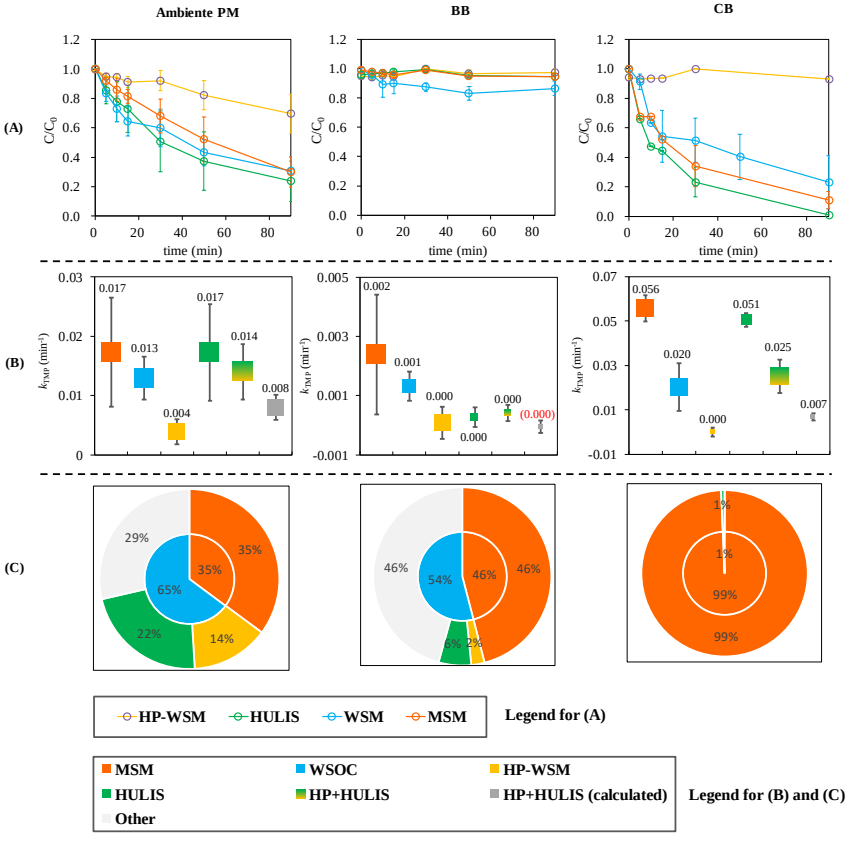

Fig.2 (A) The average attenuation curve of TMP consumption by aerosol samples of different components; (B) the triplet generation rate constant; (C) the average relative contribution to the overall triplet generation rate of the aerosol. The error bar represents one standard deviation of the experimental values of all samples.

Table 1. Formation rate constant (k_{TMP}), quantum yield coefficient (f_{TMP}) and singlet oxygen quantum yield (Φ_{1O2}) of $^3C^*$ in the different polar components of each sample.

https://doi.org/10.5194/acp-2021-842
Preprint. Discussion started: 1 November 2021

Atmospheric Chemistry and Physics Discussions

Sample number	HP-WSM			HULIS			MSM		
	k_{TMP} (min^{-1})	f_{TMP} (M^{-1})	Φ_{1O2} (%)	k_{TMP} (min^{-1})	f_{TMP} (M^{-1})	Φ_{1O2} (%)	k_{TMP} (min^{-1})	f_{TMP} (M^{-1})	Φ_{1O2} (%)
2019/12/21	0.005	51.9	6.63	0.020	89.9	4.57	0.007	0.007	7.43
2019/12/25	0.006	56.9	5.78	0.025	158.3	7.60	0.014	0.014	11.91
2020/1/3	0.005	32.0	2.78	0.013	35.6	3.43	0.018	0.018	5.40
2020/1/9	0.006	71.5	9.23	0.021	82.7	6.45	0.033	0.033	14.37
2020/1/13	0.001	5.2	5.15	0.037	167.6	4.68	0.032	0.032	7.08
2020/1/16	0.002	24.5	6.53	0.025	140.9	6.82	0.022	0.022	8.44
2020/1/18	0.006	60.4	4.39	0.013	75.8	4.60	0.007	0.007	6.76
2020/1/23	0.008	91.8	11.92	0.010	43.7	3.57	0.015	0.015	7.03
2020/1/25	0.002	39.5	3.59	0.018	102.9	5.88	0.011	0.011	6.42
2020/2/1	0.002	22.6	6.79	0.009	40.3	5.37	0.028	0.028	8.29
Wheat-straw1	0.000	0.00	3.31	0.000	4.6	1.70	0.000	0.000	4.89
Wheat-straw2	0.000	0.00	2.18	0.000	5.4	1.49	0.000	0.000	6.34
Rice-straw1	0.000	0.00	5.97	0.001	0.0	3.09	0.005	0.005	7.10
Rice-straw2	0.000	0.00	3.66	0.001	0.0	4.66	0.004	0.004	4.75
Wood1	0.001	16.3	2.45	0.000	2.0	1.95	0.001	0.001	8.80
Wood2	0.001	10.3	2.40	0.000	1.5	3.02	0.003	0.003	7.61
coal 1	0.000	3.2	1.49	0.047	270.8	38.85	0.050	0.050	25.92
coal 2	0.000	0.0	1.47	0.054	417.2	34.18	0.062	0.062	48.77
Ambient samples	0.004	45.64	6.28	0.02	93.78	5.30	0.019	0.019	8.31
(mean±SD)	±0.002	±24.54	±2.56	±0.01	±45.97	±1.31	±0.009	±0.009	±2.61
Primary samples	0-0.001	0-16.3	1.5-6.0	0-0.05	0-417	1.5-38.9	0-0.06	0-0.06	4.8-48.8
(range(mean))	(0.0002)	(3.7)	(2.9)	(0.01)	(88)	(11.1)	(0.02)	(0.02)	(14.3)

The ability to generate triplet states should be related to the chemical composition of components with different polar. The HP-WSM component has a low ability to generate triplet states, which may be related to the fact that the component contains more carboxylic acids, alcohols and sugars and other small molecules with high polarity substances, which cannot form triplet states (Bodhipaksha et al., 2015; Zhang et al., 2014). At the same time, these small molecules are also easy to quench the triplet state. The combustion sample showed different results from the actual sample (**Fig**.S13), although the particulate matter of biomass combustion has a strong light absorption capacity (Lin et al., 2017). However, in this study, the f_{TMP} all the components with different polar in the biomass combustion samples is small, and the f_{TMP} of some components is even close to zero, indicating that the light-absorbing organic matter of the biomass combustion source is not very capable of generating $^3C^*$. The HP-WSM component of the coal combustion sample has a very low

https://doi.org/10.5194/acp-2021-842
Preprint. Discussion started: 1 November 2021


Atmospheric Chemistry and Physics Discussions

ability to generate $^3C^*$, while the HULIS and MSM components have higher f_{TMP} values. Especially the HULIS component, the content of the coal sample is very small, but it has the highest generation ability of $^3C^*$ among all samples. From the results, the k_{TMP} and f_{TMP} trends of different polar components are basically the same. The difference is that the total consumption rate of TMP k_{TMP} for the MSM component is larger than that of the HULIS component, but f_{TMP} is smaller than that of HULIS, although MSM has stronger light absorption capacity than HULIS (**Fig.**S13).

Colored organics and metal ions can change their original light-absorbing characteristics through chelation (Wan et al., 2019; Kikuchi et al., 2017). Therefore, it is expected that there will be an interaction between the HP-WSM and HULIS components containing metal ions to affect the generation of triplet states. The difference between the reaction k_{TMP} value and the theoretical calculation value (the sum of the half of the respective k_{TMP} values) of the two components under the equal concentration and equal volume mixing is comparatively studied. The result is shown in **Fig.**2(B). The mixed sample consumes more TMP, and the actual environmental sample increases the generation rate of triplet by 1.8 times. This experiment demonstrates the existence of the interaction effect of photochemical reactions between different components.

According to the proportion of different polar components in the sample OC, the average contribution of different components to the total generation of $^3C^*$ is calculated, as shown in **Fig.**2(C). The contribution of the WSM component to the total k_{TMP} of PM is 65%. After separating it into single components of HP-WSM and HULIS, they contribute 14% and 22% of the triplet generation rate, respectively. Obviously, 29% has not been explained. As the result described in the previous paragraph, this is partly due to the interaction between HP-WSM and HULIS that promotes the generation of triplet states. The main possible mechanism is that the metal elements in the system chelate with certain functional groups of HULIS, forming more chromophores that can generate $^3C^*$, or reducing the energy required for the original electronic transition, thereby increasing and enhancing the generation rate of $^3C^*$. Note that this study cannot completely rule out the possibility that inorganic salt components consume TMP, such as $\cdot SO_4^-$ (Fang et al., 2013). But the experiments we added show that nitrate and sulfate do not consume TMP significantly under

https://doi.org/10.5194/acp-2021-842
Preprint. Discussion started: 1 November 2021


Atmospheric Chemistry and Physics Discussions

light conditions. There is no relevant research on the formation of $^3C^*$ from water-insoluble aerosol components. This study found that the contribution of MSM components to the formation of $^3C^*$ can reach 35% in actual samples, and even more than 99% in coal-burning samples, indicating that the contribution of water-insoluble organic carbon to aerosol triplet photochemistry is significant.

3.3 The energy distribution of triplet states of aerosols with different polarities

Different organic matter in the aerosol can form the triplet state with different energy. $^3C^*$ and O_2 in the environment can generate $^1O_2$ through energy transfer. Therefore, this study uses the Φ_{1O2} to explore the energy distribution characteristics of $^3C^*$. The experiment uses FFA as the quencher of $^1O_2$, combined with sorbic alcohol as the quencher of high-energy $^3C^*$. After adding sorbic alcohol, the calculated Φ_{1O2} is considered to be the contribution of low-energy $^3C^*$, which is different from the contribution of Φ_{1O2} when no quencher is added. The difference is considered to be the contribution of high-energy $^3C^*$, and the difference in reaction ability of $^3C^*$ with different energies is obtained (Zhou et al., 2019).

Fig.3 shows the $^3C^*$ energy distribution of different polar components. According to the results of Φ_{1O2}, the high-energy triplet states in environmental samples accounted for 3.59%-11.92%, 3.57%-7.6%, 6.08%-14.37% in HP-WSM, HULIS and MSM components, respectively. Among water-soluble components, high-energy $^3C^*$ accounts for an average of close to 80%, which is significantly higher than that of natural water (33%) and sewage (65%) samples (Zhou et al., 2019). This result is as stated in the introduction: atmospheric samples and water environment samples are quite different in terms of source and composition, and the conclusions of previous studies on the triplet state of water environment samples are not necessarily suitable for the atmospheric PM samples. In MSM, the proportion of low-energy $^3C^*$ increased, reaching an average of 52%, which should be related to the organic matter containing polycyclic conjugated electrons in the water-insoluble component. Especially for biomass combustion samples, the low-energy $^3C^*$ of different polar components has reached more than 50%. The Φ_{1O2} yield of the HP-WSM component of coal samples is very low, while the Φ_{1O2} yield of the HULIS and MSM components is the highest among all samples, reaching an average of 36% and 37%,

https://doi.org/10.5194/acp-2021-842
Preprint. Discussion started: 1 November 2021

Atmospheric Chemistry and Physics Discussions

332 respectively. Unlikeother samples, most of the coal combustion samples are contributed by
333 high-energy $^3C^*$.

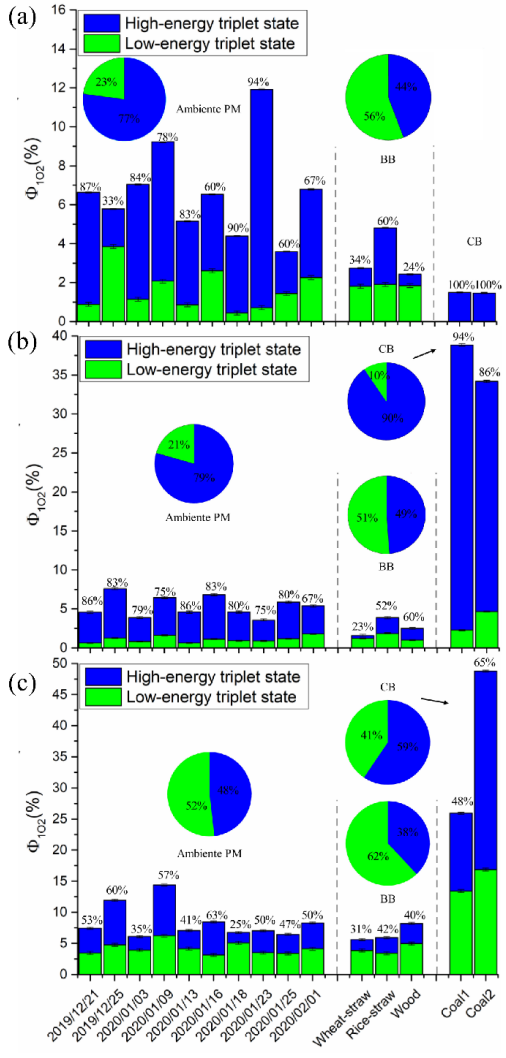

334
335 **Fig.3** $^3C^*$ energy distribution in different polar sample components. (A) Sample HP-WSM component (b)
336 Sample HULIS component (c) Sample MSM component; pie chart represents the average proportion of high and
337 low energy triplet states; the percentage represents the Φ_{1O2} caused by the high energy triplet in the total Φ_{1O2}.
338 The error bar represents one standard deviation of the experimental values of all samples.

339 High-energy $^3C^*$ has higher energy and is more reactive than low-energy $^3C^*$, and it is
340 easier to effectively collide with other substances at the molecular level. $^3C^*$ can not only
341 generate $^1O_2$, but also react with other organic substances to generate active intermediates,

https://doi.org/10.5194/acp-2021-842
Preprint. Discussion started: 1 November 2021


Atmospheric Chemistry and Physics Discussions

while the energy of low-energy $^3C^*$ only allows the conversion of O_2 to $^1O_2$. According to previous reports, among the substances that can form triplet states, aromatic ketones and other carbonyl compounds are likely to contribute a lot to high-energy $^3C^*$, while polycyclic aromatic hydrocarbons and quinones are unlikely to be the main sources of high-energy $^3C^*$ (McNeill and Canonica, 2016; Kuznetsova and Kaliya, 1992).

3.4. ROS generation caused by $^3C^*$

$^3C^*$ can induce the generation of ROS, and the ability of triplet substances with different polar components to generate ROS is different. This study uses EPR technology to identify $^1O_2$ and ·OH produced by different polar components (Blough and Zepp, 1995; Shi et al., 2003; Cote et al., 2018). The triplet quencher is used to quantitatively judge the contribution of the triplet process to the production of $^1O_2$. **Fig.**4 shows the EPR spectra of the photochemical reaction products of different components of atmospheric aerosols. It can be found that the output of $^1O_2$ is MSM>HULIS>WSM>HP-WSM, and HP-WSM is almost not detected. When the triplet quencher sorbic alcohol is added, the signal of $^1O_2$ decreases by 44%, 43% and 56%, respectively, indicating $^3C^*$ is an important precursor for the photochemical generation of $^1O_2$. This study further explored the characteristics of ·OH generated by water-soluble components under light conditions. The results showed that the EPR spectrum of the HULIS sample showed a strong ·OH signal, and the HP-WSM component also showed a certain signal. When the triplet quencher is added, the ·OH signal is significantly reduced, and the signals of each component are reduced by 59% (WSM), 75% (HULIS) and 26% (HP-WSM), respectively. This result demonstrates that $^3C^*$ is also an important precursor of ·OH. Because the methanol in the MSM sample quenched the ·OH, MSM was not tested.

The experimental results show that $^3C^*$ plays a leading role in the production of $^1O_2$ and ·OH. When there are triplet substances in the environment, the triplet state transfers energy to O_2 molecules to form $^1O_2$, and $^1O_2$ may undergo complex reactions to generate ·OH (Chen et al., 2020; Mu et al., 2020). In this study, the genertation mechanism of ·OH varies with the components. For the HP-WSM component, it contains a lot of inorganic substances such as metal ions, so it can form a Fenton-like system. For example, in the presence of H_2O_2, Fe^{2+}, Cu^{2+} will convert it into ·OH (Shi et al., 2018). For the organic

https://doi.org/10.5194/acp-2021-842
Preprint. Discussion started: 1 November 2021

Atmospheric Chemistry and Physics Discussions

component HULIS, the production of ·OH is mainly the effect of organic matter. HULIS organic matter is excited to produce $^3C^*$ and then generates $^1O_2$, and finally, $^1O_2$ leads to the formation of ·OH (**Fig.**S17). It should be noted that the possibility of triplet substances directly producing ·OH cannot be ruled out. This potential mechanism is worth exploring in the future.

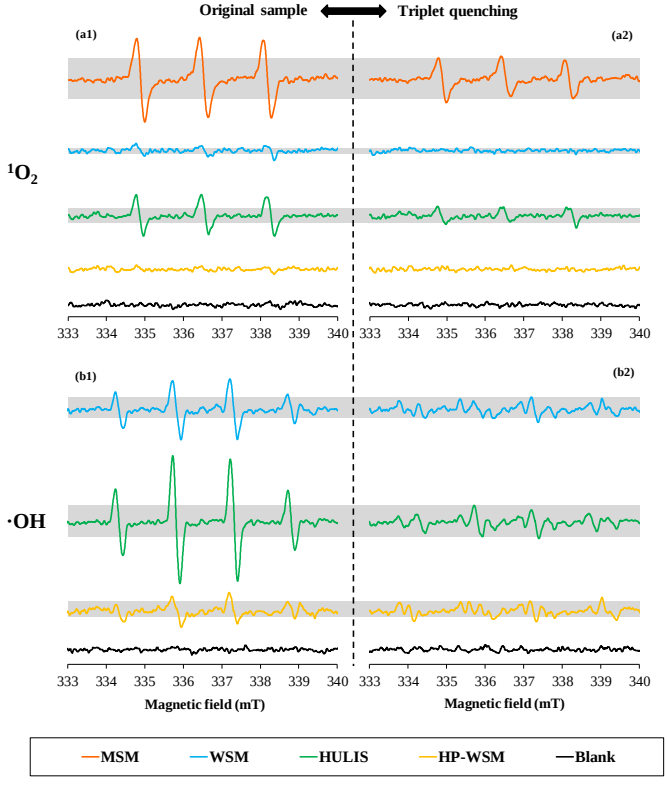

Fig.4 Different aerosol components produce (a1) singlet oxygen and (b1) hydroxyl radicals under illumination conditions, and the addition of triplet quencher (sorbic alcohol) produces (a2) singlet oxygen and (b2) hydroxyl radicals feature.

The interaction between different components also affects the photochemical generation of ROS. **Fig.**5 is the EPR signal spectrum of $^1O_2$ produced by mixing HP-WSM and HULIS (All actual atmospheric samples mixed in equal amounts). The above results have shown that the appearance of $^3C^*$ is promoted due to the interaction effect (**Fig.**2b). Furthermore, the theoretical production of $^1O_2$ should be more than half of the sum of the production of the two separate components, but **Fig.**5 shows a significant inhibitory effect

https://doi.org/10.5194/acp-2021-842
Preprint. Discussion started: 1 November 2021

Atmospheric Chemistry and Physics Discussions

that the production of $^1O_2$ is greatly reduced after mixing. This is not the expected result, and there may be a different mechanism than expected: the complex formed by metal ions and HULIS increases the total rate of $^3C^*$ formation, but it is not sensitive to the reaction pathway of energy transfer. It is easier to undergo chemical reactions through electron transfer, resulting in a decrease in the production of $^1O_2$ (McNeill and Canonica, 2016; Wan et al., 2019; Kikuchi et al., 2017; Blough and Zepp, 1995).

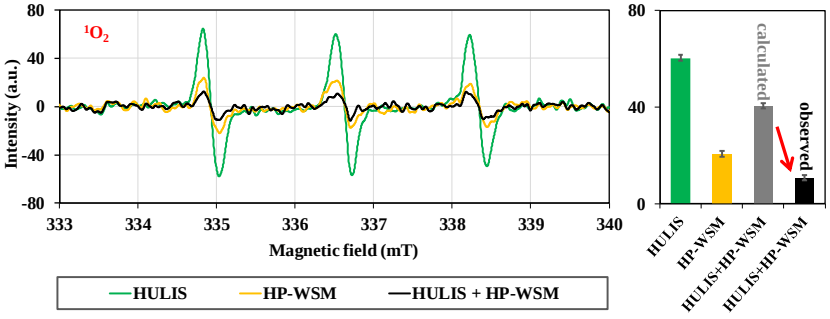

Fig.5 The mixed sample of HP-WSM and HULIS produces the EPR spectrum of $^1O_2$. The Figure shows the result of the actual atmospheric sample extract sample after 60 minutes of illumination (the signal of the control sample placed in the dark for 60 minutes has been subtracted). Reaction conditions: the mixed sample is illuminated for 60 minutes.

3.5 The relationship between optical properties and $^3C^*$ generation

The generation of $^3C^*$ should be related to optical characteristics. The study gives the absorbance and fluorescence parameters of each sample (As shown in **Table** S5 and **Fig.**S15). The results are similar to previous research reports. The non-polar components have greater light absorption and fluorescence capabilities (Chen et al., 2017). Fluorescent substances are the direct precursors for the formation of triplet states, which can be found by the correlation between k_{TMP} and standard fluorescence volume (NFV) (**Fig.**6). The sample with stronger fluorescence intensity produces $^3C^*$ at a higher rate. However, the fluorescent substances are still complex and diverse. In order to explore which chromophore is the most important triplet precursor, this study further explored the structure-activity relationship between chromophore types and triplet generation.

https://doi.org/10.5194/acp-2021-842
Preprint. Discussion started: 1 November 2021

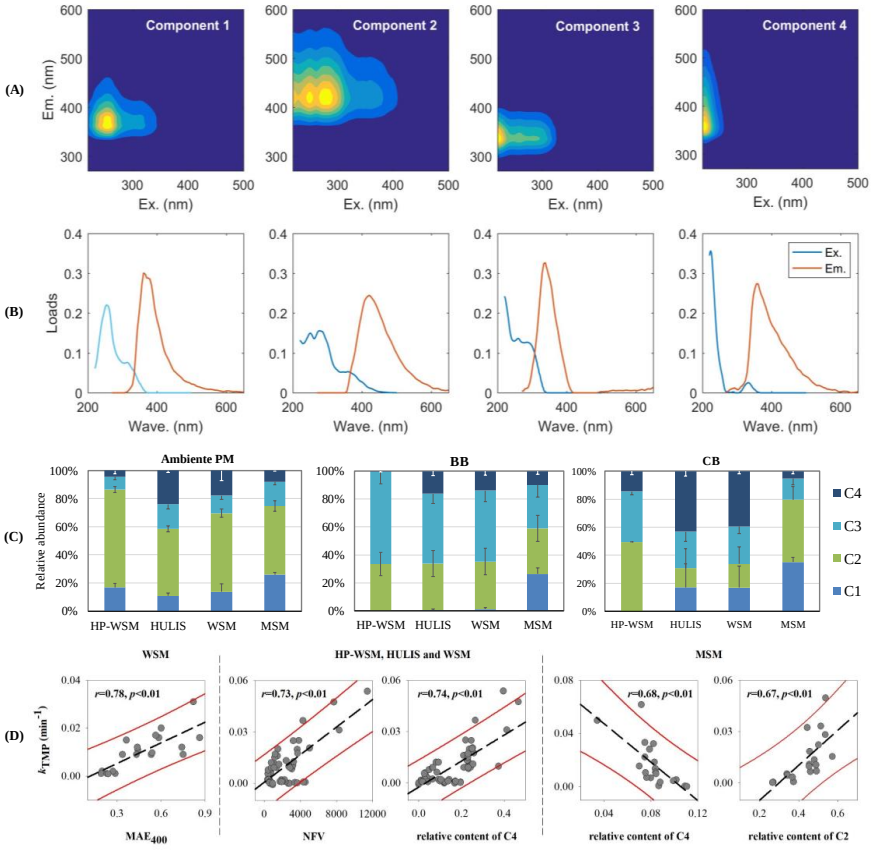

Fig.6 (a and b) The four chromophores identified and (c) the relative content in different samples and components, and (d) the correlation between MAE_{400}, NFV, C4, C2 and k_{TMP}. The error bar in the Figure (c) represents one standard deviation of all sample values; the black dashed line in the Figure (d) represents the linear fitting result, and the red line represents the 95% prediction interval.

This study identified four different chromophores C1-C4 from the samples using the EEM-PARAFAC method (**Fig.**6). Refer to previous reports that the profile of C1 is similar to low-oxidation HULIS; C2 may be highly oxidized HULIS; C3 may be Tryptophan-like OM; and C4 is similar to Tyrosine-like chromophore (Chen et al., 2021; Murphy et al., 2013; Chen et al., 2016; Chen et al., 2019). **Fig.**6(b) shows the proportions of the four chromophores in each component sample. The results show that the HULIS chromophore is the main light-absorbing organic matter in the water-soluble components, and compared with the combustion source sample, the actual aerosol contains more highly oxidized HULIS,

https://doi.org/10.5194/acp-2021-842
Preprint. Discussion started: 1 November 2021


Atmospheric Chemistry and Physics Discussions

which may be different from the actual atmospheric aerosol in the actual atmospheric environment. That is probably related to the atmospheric aging process. Tryptophan-like OM accounts for a relatively large proportion of combustion source samples. Recent studies have shown that similar chromophores may be phenolic substances (Chen et al., 2020), and biomass and coal combustion can emit a large number of phenolic substances.

The correlation between the different polar components k_{TMP} and the composition of chromophores were explored (**Fig.**6), and the correlation analysis between the quantum yield f_{TMP} and different types of chromophores was also carried out, and the results were similar to k_{TMP} Trend (**Fig.**S18). As shown in **Fig.**6, there is a positive correlation between Tyrosine-like chromophores and k_{TMP} in water-soluble components, and a negative correlation in water-insoluble components. On the contrary, among the water-insoluble components, the highly oxidized HULIS chromophore has an important role in promoting the $^3C^*$ production of the MSM component. Analogous to the related literature, this chromophore is likely to be a class of aromatic hydrocarbons containing oxygen functional groups (Zhou et al., 2017; Zhou et al., 2019), structural substances are beneficial to the formation of triplet states (**Fig.**S19). It is found that both high-energy $^3C^*$ and low-energy $^3C^*$ in the MSM component have a positive correlation with the low-oxidation HULIS chromophore, while the water-soluble component has no obvious correlation with the four chromophores, which may be due to that the triplet reaction of the chromophore is different (electron transfer and energy transfer). The low-oxidation HULIS chromophore may generate $^3C^*$ through energy transfer, while the high-oxidation HULIS chromophore is through electron transfer. For the MSM component, the triplet reaction is mainly an energy transfer type reaction. HULIS chromophores play an important role. For example, quinones may form low-energy $^3C^*$, while aromatic ketones may contribute a lot to high-energy $^3C^*$ (McNeill and Canonica, 2016; Kuznetsova and Kaliya, 1992).

4. Environmental Implications

$^3C^*$ plays an important role in the formation and aging process of atmospheric aerosols. On the one hand, $^3C^*$ itself is reactive and can directly react with other substances. On the other hand, it can produce $^1O_2$ and ·OH and other ROS substances, which indirectly

https://doi.org/10.5194/acp-2021-842
Preprint. Discussion started: 1 November 2021

Atmospheric Chemistry and Physics Discussions

participate in the generation reaction of aerosol components. In this study, the complex aerosol samples were divided into three components including HP-WSM, HULIS and MSM according to polarity, and their optical and photochemical reaction characteristics were discussed respectively. This study demonstrated that the $^3C^*$ generation characteristics of different polar components in atmospheric particulate matter samples are different. The low-polar ity components have strong light absorption and fluorescence capabilities, and the related k_{TMP} is also enhanced. Among them, the f_{TMP} of HULIS component is the strongest, and the water-insoluble components contribute the most to the total $^3C^*$ generation. This result means that the triplet photochemical reaction can enhance the heterogeneous aerosol reaction. This study also demonstrated the complexity of the triplet types. The distribution of different energy $^3C^*$ was indirectly investigated through Φ_{1O2}, and it was found that high-energy $^3C^*$ is the main form of $^3C^*$ (80%) in the water-soluble components of aerosols. The high-energy $^3C^*$ in the insoluble components accounts for 50% or even lower, and the high-energy $^3C^*$ plays a more important role in the production of $^1O_2$ and ·OH. Note that there are only few reports on the energy distribution of the triplet state of aerosols so far. Using EEM-PARAFAC technology, the structure-activity relationship between chromophore composition and triplet generation was explored, and it was found that in the water-soluble components, the chromophore previously defined as Tyrosine-like chromophore has a strong correlation with the triplet generation rate. The highly oxidized HULIS chromophore in the water-insoluble component plays an important role in promoting the production of $^3C^*$. This result means that the photochemical reaction characteristics of different chromophores are different, which ultimately determine the overall photochemical reactivity of the sample. Finally, the obtained results also proved that there is a coupling effect of photochemical reaction between HP-WSM and HULIS. After mixing, the production of $^3C^*$ is enhanced, but the production of singlet oxygen is weakened. This result means that the photochemistry of aerosol $^3C^*$ is not reacts alone, but is affected by the aerosol composition. In particular, metal ions are most likely to undergo chelation with chromophore substances, thereby changing the original optical and photochemical reaction characteristics of the chromophore. It is necessary to explore this aspect in the future.

https://doi.org/10.5194/acp-2021-842
Preprint. Discussion started: 1 November 2021

Atmospheric Chemistry and Physics Discussions

Data availability. All data that support the findings of this study are available in this article and its Supplement or from the corresponding author on request.

Supporting information. Additional information as noted in the text, including three texts (sampling information, photochemical experiment and calculation of quantum yields), six tables and nineteen **Figures** (experimental detailed data).

Author contributions. DJ and QC designed the experiments and data analysis. DJ, JW and LX performed sample collection. HL performed the EPR analysis. Other experiments are performed by DJ, YQ, XF and TC polished the article. QC prepared the paper with the contributions from all co-authors.

Competing interests. The authors declare that they have no conflict of interest.

Acknowledgments. We thank the National Natural Science Foundation of China (grant number 41877354) and the Youth Science and Technology Nova Program of Shaanxi Province (2021KJXX-36) for its financial support.

References

Arce, R., Pino, E. F., Valle, C., Agreda, J.: Photophysics and photochemistry of 1-nitropyrene, J Phys Chem A., 112, 10294-10304, https://doi.org/10294-10304, 10.1021/jp803051x, 2008.

Atkinson, R.: Atmospheric chemistry of VOCs and NOx, Atmos. Environ., 34, 2063-2101, https://doi.org/10.1016/S1352-2310(99)00460-4, 2000.

Blando, J. D., Turpin, B. J.: Secondary organic aerosol formation in cloud and fog droplets: a literature evaluation of plausibility, Atmos. Environ., 34, 1623-1632, https://doi.org/10.1016/S1352-2310(99)00392-1, 2000.

Blough, N. V., Zepp, R. G.: Reactive oxygen species in natural waters, Active Oxygen in Chemistry., 2, 280-333, https://doi.org/10.1007/978-94-007-0874-7_8, 1995.

Bodhipaksha, L. C., Sharpless, C. M., Chin, Y. P.: Triplet photochemistry of effluent and natural organic matter in whole water and isolates from effluentreceiving rivers, Environ. Sci. Technol., 49, 3453-3463, https://doi.org/10.1021/es505081w, 2015.

Canonica, S., Hellrung, B., Müller, P., Wirz, J.: Aqueous oxidation of phenylurea herbicides by triplet aromatic ketones, Environ. Sci. Technol., 40, 6636-6641, https://doi.org/10.1021/es0611238, 2006.

Chen, Q. C., Fumikazu, I., Hayato, H., Daichi, A., Michihiro, M.: Chemical structural characteristics of HULIS and other fractionated organic matter in urban aerosols: results from mass spectral and FT-IR analysis, Environ. Sci. Technol., 50, 1721-1730, https://doi.org/10.1021/acs.est.5b05277, 2016.

https://doi.org/10.5194/acp-2021-842
Preprint. Discussion started: 1 November 2021

Atmospheric Chemistry and Physics Discussions

511 Chen, Q. C., Ikemori, F., Nakamura, Y., Vodicka, P., Kawamura K., Mochida M.: Structural and light-absorption
512 characteristics of complex water-insoluble organic mixtures in urban submicrometer aerosols, Environ. Sci.
513 Technol., 51, 8293-8303, https://doi.org/10.1021/acs.est.7b01630, 2017.
514 Chen, Q. C., Li, J. W., Hua, X. Y., Jiang, X. T., Mu, Z.: Identification of species and sources of atmospheric
515 chromophores by fluorescence excitation-emission matrix with parallel factor analysis, Sci. Total. Environ.,
516 718, 137322-137332, https://doi.org/10.1016/j.scitotenv.2020.137322, 2020.
517 Chen, Q. C., Miyazaki, Y., Kawamura, K.: Characterization of chromophoric water-soluble organic matter in
518 urban, forest, and marine aerosols by HR-ToF-AMS analysis and excitation-emission matrix spectroscopy,
519 Environ. Sci. Technol., 50, 10351-10360, https://doi.org/10.1021/acs.est.6b01643, 2016.
520 Chen, Q. C., Mu, Z., Song, W.: Size-resolved characterization of the chromophores in atmospheric particulate
521 matter from a typical coal-burning city in China, J. Geophys. Res. Atmos., 124, 10546-10563,
522 https://doi.org/10.1029/2019JD031149, 2019.
523 Chen, Q. C., Mu, Z., Xu, Li.: Triplet-state organic matter in atmospheric aerosols: Formation characteristics and
524 potential effects on aerosol aging, Atmos. Environ., 252, 118343,
525 https://doi.org/10.1016/j.atmosenv.2021.118343, 2021.
526 Chow, J. C., Watson, J. G., Kuhns, H.: Source profiles for industrial, mobile, and area sources in the big bend
527 regional aerosol visibility and observational study, Chemosphere., 54, 185-208,
528 https://doi.org/10.1016/j.chemosphere.2003.07.004, 2004.
529 Cote, C. D., Schneider, S. R., Lyu, M., Gao, S., Gan, L., Holod, A. J., Chou, T. H. H., Styler, S. A.:
530 Photochemical production of singlet oxygen by urban road dust, Environ. Sci. Technol. Lett., 5, 92-97,
531 https://doi.org/10.1021/acs.estlett.7b00, 2018.
532 Dalrymple, R. M., Carfagno, R. K., Sharpless, R. M.: Correlations between dissolved organic matter optical
533 properties and quantum yields of singlet oxygen and hydrogen peroxide, Environ. Sci. Technol., 44,
534 5824-5829, https://doi.org/10.1021/es101005u, 2010.
535 De-Haan, D. O., Hawkins, L. N., Kononenko, J. A., Turley, J. J., Corrigan, A. L., Tolbert, M. A., Jimenez, J. L.:
536 Formation of nitrogen-containing oligomers by methylglyoxal and amines in simulated evaporating cloud
537 droplets, Environ. Sci. Technol., 45, 984-991, https://doi.org/10.1021/es102933x, 2010.
538 Derwent, R. G., Jenkin, M. E., Saunders, S. M., Pilling, M. J.: Photochemical ozone creation potentials for
539 organic compounds in Northwest Europe calculated with a master chemical mechanism, Atmos. Environ.,
540 32, 2429–2441, https://doi.org/10.1016/S1352-2310(98)00053-3, 1998.
541 Ervens, B., Turpin, B. J., Weber, R. J.: Secondary organic aerosol formation in cloud droplets and aqueous
542 particles (aqSOA): A review of laboratory, field and model studies, Atmos. Chem. Phys., 11, 11069-11102,
543 https://doi.org/10.5194/acp-11-11069-2011, 2011.
544 Fang, G.D., Gao, J., Dionysiou, D. D., Liu, C., Zhou, D.: Activation of persulfate by quinones: Free radical
545 reactions and implication for the degradation of PCBs, Environ. Sci. Technol., 47, 4605-4611,
546 https://doi.org/10.1021/es400262n, 2013.
547 Feczko, T., Puxbaum, H., Kasper-Giebl, A., Handler, M., Limbeck, A., Gelencser, A.: Determination of water and
548 alkaline extractable atmospheric humic-like substances with the TU Vienna HULIS analyzer in samples
549 from six background sites in Europe, J. Geophys. Res. Atmos., 112, D23S10,
550 https://doi.org/10.1029/2006JD008331, 2007.
551 Garg, S., Rose, A. L., Waite, T. D.: Photochemical production of superoxide and hydrogen peroxide from natural
552 organic matter, Geochimica Et Cosmochimica Acta., 75, 4310-4320,
553 https://doi.org/10.1016/j.gca.2011.05.014, 2011.

https://doi.org/10.5194/acp-2021-842
Preprint. Discussion started: 1 November 2021

Atmospheric Chemistry and Physics Discussions

554 Glover, C. M., Rosario-Ortiz, F. L.: Impact of halides on the photoproduction of reactive intermediates from
555 organic matter, Environ. Sci. Technol., 47, 13949-13956, https://doi.org/10.1021/es4026886, 2013.
556 Goldstein, A. H., Galbally, I. E.: Known and unexplored organic constituents in the earth's atmosphere, Environ.
557 Sci. Technol., 41, 1514-1521, https://doi.org/10.1021/es072476p, 2007.
558 Griffith, E. C., Carpenter, B. K., Shoemaker, R. K., Vaida, V.: Photochemistry of aqueous pyruvic acid, P Natl
559 Acad Sci., 110, 11714-11719, https://doi.org/10.1073/pnas.1303206110, 2013.
560 Hawkins, L. N., Welsh, H. G., Alexander, M. V.: Evidence for pyrazine-based chromophores in cloud water
561 mimics containing methylglyoxal and ammonium sulfate, Atmos. Chem. Phys., 18, 12413-12431,
562 https://doi.org/10.5194/acp-18-12413-2018, 2018.
563 Halladja, S., Ter-Halle, A., Aguer, J. P.: Inhibition of humic substances mediated photooxygenation of furfuryl
564 alcohol by 2,4,6-trimethylphenol: Evidence for reactivity of the phenol with humic triplet excited states,
565 Environ. Sci. Technol., 41, 6066-6073, https://doi.org/10.1021/es070656t, 2007.
566 Herrmann, H., Schaefer, T., Tilgner, A., Styler, S. A., Weller, C., Teich, M., Otto, T.: Tropospheric aqueous-phase
567 chemistry: Kinetics, mechanisms, and its coupling to a changing gas phase, Chem. Rev., 115, 4259-4334,
568 https://doi.org/10.1021/cr500447k, 2015.
569 Kaur, R., Anastasio, C.: First measurements of organic triplet excited states in atmospheric waters. Environ, Sci.
570 Technol., 52, 5218-5226, https://doi.org/10.1021/acs.est.7b06699, 2018.
571 Kellogg, R. E., Simpson, W. T.: Perturbation of singlet-triplet transition energies, J. Am. Chem. Soc., 87,
572 4230-4234, https://doi.org/10.1021/ja00947a002, 1965.
573 Kikuchi, T., Fujii, M., Terao, K., Jiwei, R., Lee, Y. P., Yoshimura, C.: Correlations between aromaticity of
574 dissolved organic matter and trace metal concentrations in natural and effluent waters: A case study in the
575 Sagami River Basin, Japan, Sci. Total Environ., 576, 36-45, https://doi.org/10.1016/j.scitotenv.2016.10.068,
576 2017.
577 Kuznetsova, N. A., Kaliya, O. L.: The photochemistry of coumarins, Chem. Rev., 61, 683-696,
578 https://doi.org/10.1070/RC1992v061n07ABEH000992, 1992.
579 Laskin, A., Laskin, J., Nizkorodov, S.: Chemistry of atmospheric brown carbon, Chem. Rev., 115, 4335-4382,
580 https://doi.org/10.1021/cr5006167, 2015.
581 Lee, H. J., Aiona, P. K., Laskin, A., Laskin, J., Nizkorodov, S. A.: Effect of solar radiation on the optical
582 properties and molecular composition of laboratory proxies of atmospheric brown carbon, Environ. Sci.
583 Technol., 48, 10217-10226, https://doi.org/10.1021/es502515r, 2014.
584 Lim, H. J., Carlton, A. G., Turpin, B. J.: Isoprene forms secondary organic aerosol through cloud processing:
585 Model simulations. Environ, Sci. Technol., 39, 4441-4446, https://doi.org/10.1021/es048039h, 2005.
586 Lin, P., Bluvshtein, N., Rudich, Y., Nizkorodov, S. A., Laskin, J., Laskin, A.: Molecular chemistry of atmospheric
587 brown carbon inferred from a nationwide biomass burning event. Environ, Sci. Technol., 51, 11561-11570,
588 https://doi.org/10.1021/acs.est.7b02276, 2017.
589 Lin, P., Rincon, A. G., Kalberer, M., Yu, J. Z.: Elemental composition of HULIS in the Pearl River Delta Region,
590 China: Results inferred from positive and negative electrospray high resolution mass spectrometric data,
591 Environ. Sci. Technol., 46, 7454-7462, https://doi.org/10.1021/es300285d, 2012.
592 McNeill, K., Canonica, S.: Triplet state dissolved organic matter in aquatic photochemistry: Reaction
593 mechanisms, substrate scope, and photophysical properties, Environ. Sci. Proc. Imp., 18, 1381-1399,
594 https://doi.org/10.1039/c6em00408c, 2016.
595 Mostafa, S., Rosario-Ortiz, F. L.: Singlet oxygen formation from wastewater organic matter, Environ. Sci.
596 Technol., 47, 8179-8186., https://doi.org/10.1021/es401814s, 2013.

https://doi.org/10.5194/acp-2021-842
Preprint. Discussion started: 1 November 2021

Atmospheric Chemistry and Physics Discussions

597 Murphy, K. R., Stedmon, C. A., Graeber, D.: Fluorescence spectroscopy and multi-way techniques-PARAFAC,
598 Anal. Methods., 5, 6557-6566, https://doi.org/10.1039/c3ay41160e, 2013.
599 Mu, Z., Chen, Q. C., Zhang, L. X., Guan, D. J., Li, H.: Photo-degradation of atmospheric chromophores: Type
600 conversion and changes in photochemical reactivity, Atmos. Chem. Phys. Discuss.,[preprint],
601 https://doi.org/10.5194/acp-2020-1223, in review, 2020.
602 Nguyen, Q. T., Kristensen, T. B., Hansen, A. M. K., Skov, H., Bossi, R., Massling, A., Sørensen, L. L., Bilde, M.,
603 Glasius, M., Nøjgaard, J. K.: Characterization of humic-like substances in Arctic aerosols, J. Geophys. Res.
604 Atmos., 119, 5011-5027, https://doi.org/10.1002/2013JD020144, 2014.
605 Parker, K. M., Pignatello, J. J., Mitch, W. A.: Influence of ionic strength on tripletstate natural organic matter loss
606 by energy transfer and electron transfer pathways, Environ. Sci. Technol., 47, 10987-10994,
607 https://doi.org/10.1021/es401900j, 2013.
608 Perri, M. J.; Seitzinger, S. P.; Turpin, B. J. Secondary organic aerosol production from aqueous photooxidation of
609 glycolaldehyde:Laboratory experiments. Atmos. Environ. 2009, 43, 1487-1497.
610 Rollins, A. W., Browne, E. C., Min, K. E., Pusede, S. E.: Evidence for NOx control over nighttime SOA
611 formation, Science., 337, 1210-1212, https://doi.org/10.1126/science.1221520, 2012.
612 Rincon, A. G., Guzman, M. I., Hoffmann, M. R., Colussi, A. J. J.: Optical absorptivity versus molecular
613 composition of model organic aerosol matter, Phys. Chem. A., 113, 10512-10520,
614 https://doi.org/10.1021/jp904644n, 2009.
615 Shi, T. M., Schins, R. P. F., Knaapen, A. M.; Kuhlbusch, T., Pitz, M., Heinrich, J., Borm, P. J. A.: Hydroxyl
616 radical generation by electron paramagnetic resonance as a new method to monitor ambient particulate
617 matter composition, J. Environ. Monit., 5, 550-556, https://doi.org/10.1039/B303928P, 2003.
618 Vione, D., Maurino, V., Minero, C., Pelizzetti, E., Harrison, M. A. J.: Photochemical reactions in the tropospheric
619 aqueous phase and on particulate matter, Chem. Soc. Rev., 35, 441-453, https://doi.org/10.1039/b510796m,
620 2006.
621 Vione, D., Minella, M., Maurino, V., Minero, C.: Indirect photochemistry in sunlit surface waters: Photoinduced
622 production of reactive transient species, Chem. Eur. J., 20, 10590-10606,
623 https://doi.org/10.1002/chem.201400413, 2014.
624 Wang, Y. J., Hu, M., Lin, P., Guo, Q. F., Wu, Z. J., Li, M. R., Zeng, L. M., Song, Y., Zeng, L. W., Wu, Y. S., Guo,
625 S., Huang, X. F., He, L. Y.: Molecular characterization of nitrogen-containing organic compounds in
626 humic-like substances emitted from straw residue burning, Environ. Sci. Technol., 51, 5951-5961,
627 https://doi.org/10.1021/acs.est.7b00248, 2017.
628 Wan, D., Sharma, V. K., Liu, L., Zuo, Y. G., Chen, Y.: Mechanistic insight into the effect of metal ions on
629 photogeneration of reactive species from dissolved organic matter, Environ. Sci. Technol., 53, 5778-5786,
630 https://doi.org/10.1021/acs.est.9b00538, 2019.
631 Warneck, P.: The relative importance of various pathways for the oxidation of sulfur dioxide and nitrogen dioxide
632 in sunlit continental fair weather clouds, Phys. Chem. Chem. Phys., 1,
633 5471-5483, https://doi.org/10.1039/A906558J, 1999.
634 Wenk, J., Von, G. U., Canonica, S.: Effect of dissolved organic matter on the transformation of contaminants
635 induced by excited triplet states and the hydroxyl radical, Environ. Sci. Technol., 45, 1334-1340,
636 https://doi.org/10.1021/es102212t, 2011.
637 Wilkinson, F., Helman, W. P., Ross, A. B.: Quantum yields for the photosensitized formation of the lowest
638 electronically excited singlet state of molecular oxygen in solution, J. Phys. Chem. Ref. Data., 22, 113-262,
639 https://doi.org/10.1063/1.555934, 1993.

https://doi.org/10.5194/acp-2021-842
Preprint. Discussion started: 1 November 2021

Atmospheric Chemistry and Physics Discussions

640 Xu, H. M., Cooper, W. J., Jung, J. y., Song, W. H.: Photosensitized degradation of amoxicillin in natural organic
641 matter isolate solutions, Water Res., 45, 632-638, https://doi.org/10.1016/j.watres.2010.08.024 ,2011.
642 Zhang, D. N., Yan, S. W., Song, W. H.: Photochemically induced formation of reactive oxygen species (ROS)
643 from effluent organic matter, Environ. Sci. Technol., 48, 12645-12653, http://dx.doi.org/10.1021/es5028663,
644 2014.
645 Zhou, H. X., Yan, S. W., Ma, J. Z., Lian, L. S., Song, W. H.: Development of novel chemical probes for
646 examining triplet natural organic matter under solar illumination, Environ. Sci. Technol., 51,
647 http://dx.doi.org/10.1021/acs.est.7b02828, 11066-11074, 2017a.
648 Zhou, H. X., Lian, L. S., Yan, S.W., Song, W. H.: Insights into the photo-induced formation of reactive
649 intermediates from effluent organic matter: the role of chemical constituents, Water Res., 112, 120-128,
650 http://dx.doi.org/10.1016/j.watres.2017.01.048, 2017b.
651 Zhou, H. X., Yan, S. W., Lian, L. S., Song, W. H.: Triplet-state photochemistry of dissolved organic matter:
652 triplet-state energy distribution and surface electric charge conditions, Environ. Sci. Technol., 53, 2482-2490,
653 http://dx.doi.org/10.1021/acs.est.8b06574, 2019.